M-shell ionization resulting from near-central collisions of mid-*Z* atoms with 5.5-MeV/amu oxygen ions

M. W. Carlen,* B. Boschung, J.-Cl. Dousse, Z. Halabuka, J. Hoszowska, J. Kern, and Ch. Rhême
Physics Department, University of Fribourg, CH-1700 Fribourg, Switzerland

M. Polasik
Institute of Chemistry, Nicholas Copernicus University, 87-100 Torun, Poland

P. Rymuza and Z. Sujkowski
Institute for Nuclear Studies, 05-400 Swierk, Poland

(Received 28 December 1992; revised manuscript received 26 August 1993)

The $K\alpha$ and $K\beta$ x-ray spectra of palladium and lanthanum bombarded by 5.5-MeV/amu ^{16}O ions were measured with a high-resolution transmission crystal spectrometer. The observed complex structure of the $K\alpha L^0$ and $K\beta_{1,3}L^0$ lines consisting of many M satellites was analyzed by means of theoretical line profiles based on multiconfiguration Dirac-Fock calculations. The average M-shell and M-subshell ionization probabilities in near-central collisions are determined. The experimental results are compared to the predictions of the semiclassical-approximation theory. The agreement is much improved by using Dirac-Hartree-Fock (DHF) wave functions instead of screened relativistic hydrogenic wave functions. The importance of DHF wave functions in the calculation of the M-shell ionization probabilities is illustrated with other examples.

PACS number(s): 34.50.Fa, 32.30.Rj, 35.80.+s

I. INTRODUCTION

The aim of the present study is to contribute to the understanding of the ionization mechanism in near-central collisions of energetic heavy ions with atoms. In the past few decades great interest has been devoted to the inner-shell ionization processes [1]. While not yet satisfactory, the knowledge about the ionization of the K and L shells is far better [2–6] than for the M shell. Data for the M-shell ionization cross sections [7–11] and data for the impact-parameter-dependent M-shell ionization probabilities are scarce and difficult to obtain.

Generally, ionization cross sections are determined by measuring the x-ray or Auger production cross sections and converting them to ionization cross sections by using fluorescence, Auger and Coster-Kronig yields. These yields have rather large uncertainties which reflect the errors of the final cross-section values. Further problems arise from the complexity of the L and M x-ray spectra, from their low energies and from target contaminations. For the M-shell ionization, discrepancies up to a factor of 2 are observed between the experimental data reported by different authors [9].

The impact-parameter dependence of the ionization probability is expected to be more useful to test ionization theories and the behavior of the wave functions during the collision than the total ionization cross sections. To our knowledge, a measurement of the differential M-shell ionization cross section has not yet been attempted in view of large experimental difficulties. In Ref. [12] we presented a new way for determining the M-shell ionization probability in near-central collisions. Using a high-resolution crystal spectrometer in DuMond geometry [13] we were able to separate the diagram and the L-satellite K x-ray lines of a Mo target bombarded with ^4He ions. For the $K\beta_2$ transition, the M satellites could also be resolved. Assuming the independent-particle model without any correlations [14–16] it was possible to deduce the ionization probabilities from the measured satellite intensity ratios. Because the latter are only weakly influenced by the uncertainties of the fluorescence and Coster-Kronig yields, accurate results could be obtained. In Ref. [17] a similar experiment, performed with Pd and La targets was described. A comparison with theoretical ionization probabilities, calculated with the semiclassical approximation using screened relativistic hydrogenic wave functions, showed discrepancies up to a factor of 4 and more. The deviations increased with increasing reduced velocities.

For heavier projectiles the structure of the x-ray spectra becomes much more complex, since due to the ion-atom collision several electrons are ejected simultaneously resulting in multiply ionized target atoms. A correct analysis of the x-ray spectra is then difficult and the theoretical knowledge of line profiles is needed, which require calculated x-ray energies and transition probabilities. In Ref. [18] an alternative method for the analysis of such complex spectra was presented and applied to the $K\alpha$ and $K\beta$ spectra of Mo bombarded by 5.5-MeV/amu oxygen ions. The comparison of the measured M-shell

*Present address: NREL, 1617 Cole Boulevard, Golden, CO 80401-3393.

ionization probability with the one calculated within the semiclassical approximation (SCA) model showed again a discrepancy of a factor of 3.

In this paper we apply our method of analysis to the K x-ray spectra of Pd and La targets bombarded with 5.5-MeV/amu oxygen ions. The resulting M-shell ionization probabilities in near-central collisions are compared with new SCA calculations using more realistic Dirac-Hartree-Fock wave functions instead of screened relativistic hydrogenlike wave functions. A satisfactory agreement is obtained.

For the K and L shells relativistic hydrogenic wave functions are, in general, suitable. For the M shell, due to the larger influence of screening, a better approximation is needed. The M shell is thus a good probe to assess the importance of the choice of the proper wave functions in SCA calculations.

II. EXPERIMENT

An in-beam bent-crystal spectrometer in the modified DuMond slit geometry, installed at the PSI variable-energy cyclotron in Villigen, Switzerland, was used for the high-resolution study of the palladium and lanthanum spectra. The spectrometer and the experimental setup were described in detail elsewhere [13,12]. The spectrometer was equipped with quartz-crystal plates of 1.5 or 2.5 mm thickness and a 1-mm-thick Na(Tl) detector, surrounded by an anti-Compton ring. The radius of curvature of the crystals was 3.15 m. A high-frequency alternating electric field was applied to the crystals [19], enhancing the peak reflectivity by a factor of 3–4. Targets of natural Pd and La about 15 mg/cm^2 thick were bombarded by 112-MeV ^{16}O ions. Beam intensities of about 100 nA were used. The beam intensity was monitored by observing the target $K\alpha$ x rays with a 6-cm^3 Ge(Li) detector. The ions were fully stripped by passing the 4.4 mg/cm^2 Havar entrance window of the target chamber. The target was cooled by a low-pressure He gas flow, pumped through the target chamber. Taking into account the energy loss in the Havar foil, the self-absorption and stopping power of the target, and the energy dependence of the K-shell ionization cross section, the effective beam energy for producing the observed x rays was about 5.5 MeV/nucleon.

The instrumental resolution and the line shape were obtained by measuring the 25.7-keV γ-ray line of a radioactive ^{161}Tb source, placed 30 cm behind the target and observed through the slit. The instrumental resolution was comparable to the natural linewidth of the K x-ray lines. According to Salem and Lee [20] the Lorentzian width of the $K\alpha$ transitions is about 9 eV for Pd and 18 eV for La, respectively, and about 8.5 eV (Pd) and 19.5 eV (La) for the $K\beta$ transitions. The full width at half maximum of the Gaussian, representing the instrumental line shape, was 11 eV for the $K\alpha$ and $K\beta$ transitions of Pd, 25 eV for the La $K\alpha$ transitions, and 32 eV for the La $K\beta$ transitions. The energy calibrations are based on the 48.915 62(14) keV and the 74.567 11(22) keV γ-ray lines [21] in the ^{161}Tb decay, measured in second order on both sides of reflection.

As a result of the shift towards higher energies of the satellite transitions with respect to the diagram ones, a part of the measured $K\beta$ spectrum lies above the K edge, which is at 24.3503 keV for Pd and 38.9246 keV for La [22]. For this part of the spectrum the self-absorption in the target is strongly increased. Taking into account the dependence of the ionization cross section on the projectile energy, the measured intensities of this region of the spectrum were multiplied by a factor of 1.4(0.2) for Pd and 1.2(0.1) for La, after substraction of the background.

III. DESCRIPTION OF THE METHOD OF ANALYSIS

The measured Pd and La K x-ray spectra are shown in Fig. 1. In an energetic heavy ion-atom collision, multiple inner-shell ionization is an important fact. Since the removal of electrons modifies the screening of the nuclear charge, the x-ray transitions of a multiply ionized atom (x-ray satellite transitions) are shifted in energy with respect to the energy of the diagram transitions. The energy shifts depend on the subshells where the holes are located. Therefore the $K\alpha$ x-ray spectrum of a multiply

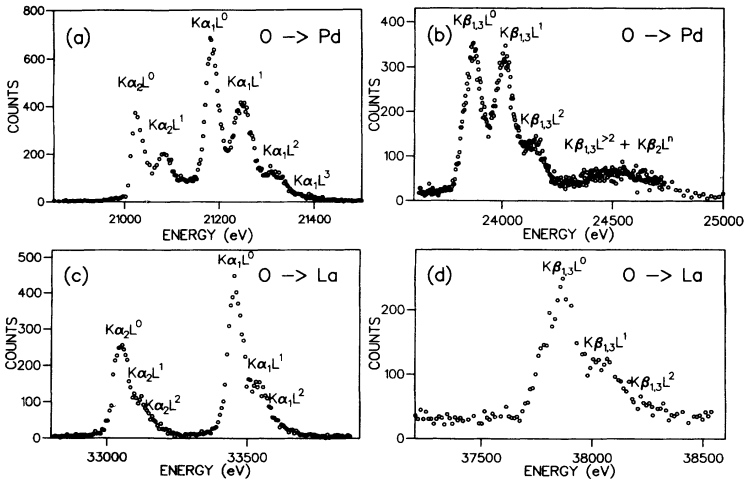

FIG. 1. High-resolution crystal spectrometer $K\alpha$ and $K\beta$ x-ray spectra of palladium and lanthanum. (a) 5.5-MeV/amu ^{16}O-induced $K\alpha$ spectrum of Pd. (b) 5.5-MeV/amu ^{16}O-induced $K\beta$ spectrum of Pd. (c) 5.5-MeV/amu ^{16}O-induced $K\alpha$ spectrum of La. (d) 5.5-MeV/amu ^{16}O-induced $K\beta$ spectrum of La.

ionized atom consists not of two single lines ($K\alpha_1$ and $K\alpha_2$) but of several lines with dozens or hundreds of unresolved components. Taking into account the different coupling possibilities of the angular momenta j of the open subshells, a x-ray line can be composed of many thousands of components and can have a very complex structure. The energy shift for a satellite x-ray transition decreases with the principal quantum number of the spectator vacancy and is higher for $K\beta$ than for $K\alpha$ transitions. Depending on the shifts and on the instrumental and natural widths, well-resolved peaks or, on the contrary, broadened bumps are observed in the measured spectra. This can be seen in Fig. 1: for Pd the L-satellite x rays (x-ray transitions with one or several additional holes in the L shell) are well resolved, for La the resolution is just at the limit. In both cases is it not possible to resolve the M satellites, the peaks being strongly broadened and somewhat shifted. However, in the case of weakly ionizing projectiles like He ions, and for the $K\beta_2$ ($N_{\mathrm{II,III}} \rightarrow K$) transitions, it was shown that it is possible to resolve also the M satellites [12,17].

As mentioned in the Introduction, this paper deals with M-shell ionization. Since the individual $K\alpha M^m$ and $K\beta M^m$ satellites cannot be resolved, a detailed analysis is necessary. A trustworthy analysis is only possible if one knows the M-satellite structure underlying the broadened peaks. We will use the new method proposed in Ref. [18] for the analysis of the K x-ray spectra of multiply ionized mid-Z atoms, which are produced in near-central collisions with energetic heavy projectiles. In the following we give a short description of this method.

The measured $K\alpha$ and $K\beta$ lines are assumed to be linear combinations of all possible $K\alpha L^n M^m$ and $K\beta L^n M^m$ profiles. The latter are constructed theoretically using transition energies and transition probabilities determined by extensive multiconfiguration Dirac-Fock (MCDF) calculations. Assuming a binomial distribution (see Secs. IV and V) of holes in the M shell and treating the M-shell ionization probabilities as adjustable parameters, the measured $K\alpha$ and $K\beta$ spectra are simultaneously decomposed into these theoretically constructed shapes. The MCDF method employed in the present study has been described in detail in several papers [23–28].

In the present study we used the computer program package GRASP [29], which allows relativistic MCDF calculations with the inclusion of the transverse (Breit) interaction and QED (self-energy and vacuum polarization) corrections. Transition energies and probabilities were calculated using the modified special average level version [30] of MCDF with the same factors λ as in Ref. [18]. The jj coupling scheme was applied. The coupling of the open subshells produces many initial and final states and herewith the number of x-ray transitions increases very rapidly. The $K\alpha$ spectrum of an atom with full outer subshells (e.g., Pd) consists of two diagram lines. One spectator vacancy in the L shell raises the number of transitions to 20, and two vacancies to 84. The $K\alpha L^0 M^1$ complex consists of 72 components and the $K\alpha L^0 M^2$ one consists of 1697. For $K\alpha L^1 M^1$ one has 996 components and for $K\alpha L^1 M^2$ more than 16 500. Practically it is thus only possible to calculate the $K\alpha L^0 M^m$ but not all $K\alpha L^n M^m$ ($n \geq 1$) satellite transitions. For the analysis of the M-shell ionization this is enough, since the M-shell hole distribution and therefore the M-shell ionization probability are contained in the L^0 peak. Calculated average energy shifts due to several M-shell holes are given in Table I.

An essential point of the method is the simultaneous fit of the $K\alpha$ and $K\beta$ spectra. Only in this way can reliable results be obtained. Since the energy shifts of the satellites are different for $K\alpha$ and $K\beta$, this puts a strong condition for the fit to find the correct parameters [18].

By folding the Lorentzian natural line shape with the Gaussian instrumental response and using the calculated energies and transition probabilities the shapes of the $KL^0 M^m$ lines were constructed. Assuming a binomial distribution of the M-shell holes, the $KL^0 M^m$ lines were combined to form the $K\alpha L^0$ and $K\beta L^0$ peaks. The binomial distribution is governed by a single parameter p_M, which is the probability per M-shell electron at the moment of the K x-ray transition. This parameter is common for all subshells and represents an average value. The envelope of the theoretically constructed $K\alpha L^0$ and $K\beta L^0$ peaks are fitted to the measured K x-ray spectra. The L^1 satellites and also for Pd $K\alpha$ the L^2 satellites were taken into account in the fitting procedure as single peaks with larger Gaussian widths. The only free parameters in the fit were p_M^x, the background level, and an intensity scaling factor.

The calculated energy shifts are different for holes in different subshells. The shifts due to $3s$ (M_{I}) and $3p$

TABLE I. Calculated average energy shifts (eV) of $K\alpha M^m$ and $K\beta_{1,3} M^m$ x-ray satellite transitions of Pd and La in comparison with the instrumental (σ) and natural (Γ) widths (eV).

Number of M holes or width	Pd			La		
	$K\alpha_1$	$K\alpha_2$	$K\beta_{1,3}$	$K\alpha_1$	$K\alpha_2$	$K\beta_{1,3}$
M^1	3.9	3.2	15.5	3.1	7.3	24.7
M^2	6.9	6.3	31.6	10.8	10.1	50.0
M^3	10.2	9.0	48.3	16.2	14.5	77.3
M^4	13.6	12.2	65.7	21.2	19.3	103.3
σ	11.0	11.0	11.0	25.0	25.0	32.0
Γ	8.8	9.2	8.5	17.4	18.1	19.5

TABLE II. Calculated energy shifts (eV) of the Pd and La M x-ray satellite transitions with respect to the diagram lines due to a hole in the different M subshells.

	ΔE	
Transition	Pd	La
$K\alpha_1 M_I^1$	5.7	9.1
$K\alpha_1 M_{II,III}^1$	10.4	14.9
$K\alpha_1 M_{IV,V}^1$	−0.5	−4.1
$K\alpha_2 M_I^1$	5.7	8.6
$K\alpha_2 M_{II,III}^1$	8.9	12.9
$K\alpha_2 M_{IV,V}^1$	−0.8	1.8
$K\beta_{1,3} M_I^1$	20.4	31.0
$K\beta_{1,3} M_{II,III}^1$	19.4	30.1
$K\beta_{1,3} M_{IV,V}^1$	12.4	20.8

($M_{II,III}$) holes are similar, but for the $3d$ ($M_{IV,V}$) holes they are different (see Table II and [31]). Since the wave functions of the M subshells are rather different, one can expect the ionization probabilities to also be distinct. Therefore, in a further step, the analysis was performed by using two different probabilities: one, p_{3sp}^X, common for the $3s$ and $3p$ subshells and another, p_{3d}^X, for the $3d$ subshells. Assuming again binomial distributions for the M-subshell holes the $K\alpha L^0(3sp)^{m1}(3d)^{m2}$ and $K\beta_{1,3}L^0(3sp)^{m1}(3d)^{m2}$ lines were fitted to the measured spectra and the two probabilities p_{3sp}^X and p_{3d}^X were determined.

For the MCDF calculation of La with the GRASP code, a modification of the experimental electron configuration had to be made. The experimental electron configuration of La is $5s^25p^65d^16s^2$ and the atom has therefore one open subshell in the ground state. The number of coupling possibilities increases very rapidly with the addition of spectator holes so that a calculation is practically no longer possible. Therefore the outer electron in the $5d$ subshell was neglected and the ground state was assumed to be $5s^25p^65d^06s^2$, corresponding to a singly ionized atom with full subshells. Since the $5d$ electron is only weakly bound, its influence on the K x-ray transitions is very small and the calculated transition energies are almost not affected (see Table III). For Pd, the correct $4s^24p^64d^{10}$ electron configuration was used for the calculation.

IV. RESULTS

The uncorrelated direct Coulomb ionization of the atomic electrons in the independent-particle picture can be described by a binomial distribution with the ionization probability per electron as parameter. The cross section for the production of 1 K-shell and m M-shell holes is

$$\sigma_{KM^m}=2\pi\int_0^{b_{\max}} db\, b \begin{bmatrix}2\\1\end{bmatrix} p_K(b)[1-p_K(b)] \times \sum_{\Sigma k_i=m} \prod_{i=1,5} \begin{bmatrix}m_i\\k_i\end{bmatrix} p_{M_i}^{k_i}(b) \times [1-p_{M_i}(b)]^{m_i-k_i}, \quad (1)$$

where b is the impact parameter, $p_K(b)$ is the impact-parameter-dependent ionization probability per K-shell electron, $p_{M_i}(b)$ is the M_i-subshell ionization probability per electron, and m_i is the number of electrons in the M subshells. If the M_i-subshell ionization probabilities do not differ much, an average ionization probability for the M shell can be defined and Eq. (1) can be written as

$$\sigma_{KM^m}=2\pi\int_0^{b_{\max}} db\, b \begin{bmatrix}2\\1\end{bmatrix} p_K(b)[1-p_K(b)] \times \begin{bmatrix}18\\m\end{bmatrix} p_M^m(b)[1-p_M(b)]^{18-m}. \quad (2)$$

$b_{\max}$ is given by the condition that for $b>b_{\max}$, $p_K(b)$ is negligibly small and the integral remains almost constant. The main contribution to the integral comes from the impact parameters $b\approx 500$ fm. In the impact-parameter range $b=[0,b_{\max}]$, $p_M(b)$ is nearly constant: $p_M(b<b_{\max})\approx p_M(500\text{ fm})$ and the cross section behaves as a binomial distribution

$$\sigma_{KM^m}\propto \begin{bmatrix}18\\m\end{bmatrix} p_M^m(500)[1-p_M(500)]^{18-m}. \quad (3)$$

In order that the measured vacancy distribution can be represented by a binomial distribution two conditions have to be met. First, ionizing processes other than direct Coulomb ionization as electron capture, electron shake off, or target activation have to be negligible or small (see Sec. V). Second, competing decay processes to the K x rays (L and M Auger, Coster-Kronig, and radiative transitions) have to play a minor role (see Secs. IV B and IV D). In our case, the influence of both factors is small and the assumption of a binomial distribution is in a first approximation justified.

We would like to mention at this point a further effect

TABLE III. Calculated (E_{calc}) and standard (E_{Bearden}) (Ref. [66]) K x-ray energies in eV for Pd and La. The electron configuration of Pd was $4s^24p^64d^{10}$. For La the configuration $5s^25p^65d^06s^2$ of the singly ionized atom was used for the ground state (see text).

	Pd		La	
Transition	E_{calc}	E_{Bearden}	E_{calc}	E_{Bearden}
$K\alpha_2$	21020.3	21020.1(1)	33033.2	33034.1(2)
$K\alpha_1$	21177.1	21177.1(1)	33440.4	33441.8(2)
$K\beta_3$	23791.4	23791.1(2)	37718.0	37720.2(5)
$K\beta_1$	23819.2	23818.7(2)	37798.6	37801.0(3)

which may influence and change the M-shell vacancy distribution prior to the K x-ray decay: interatomic electron transfer. A comparison of heavy-ion-induced $K\alpha$ satellite x-ray spectra of solid and gaseous fluorine ($Z=9$) compounds showed that for solid compounds the L-vacancy filling prior to K-vacancy decay occurs with a probability of almost 1 for highly ionized states [32]. For third-row target atoms, where the L-shell electrons are not valence electrons, the effect is of the order of 5% [33,34]. Rossel *et al.* [35] investigated the effect of the different chemical environment on the L x-ray satellite transitions of molybdenum compounds and alloys and found differences in the intensity yields of $L\alpha$ and $L\beta_1$ M satellites, which were correlated with the valence electron density. For Pd and La, to our knowledge, no gas-solid target comparison data exist. An estimation of the order of magnitude of interatomic transitions to the target M shell is difficult and further investigation is needed. Nevertheless, since for Pd and La the M shell is an inner shell and the K x-ray transitions are very fast ($\sim 10^{-16}$ s), the change of the M-shell vacancy distribution due to interatomic electron transfer is expected to be small and was therefore neglected. Substantial interatomic transition probabilities would cause an underestimation of the M-shell ionization probability at the moment of the ion-atom collision p_M.

A. Average M-shell ionization at the moment of the K x-ray emission

For the determination of the average M-shell ionization probability per electron at the moment of the K x-ray emission p_M^x the $K\alpha_1 L^0$, $K\alpha_2 L^0$, and $K\beta_{1,3} L^0$ peaks have been analyzed. The intensities of the L^n ($n \geq 1$) satellites were fixed. They have been determined by using the method described in Ref. [18]. Briefly, the energies and probabilities of the $K\alpha L^n M^0$, $K\beta_{1,3} L^n M^0$, and $K\beta_2 L^n M^0$ transitions were calculated with the GRASP code [29] and the theoretical line shape was constructed by folding a Gaussian with a Lorentzian and summing up all the components. The effect of the M-shell holes was taken into account by using a larger Gaussian width than the instrumental one and shifting the center of gravity of the lines. The Gaussian widths, the shifts of the lines, and the L^n peak intensities were then free parameters in the fit.

The simultaneous fit of the $K\alpha_{1,2} L^0$ and the $K\beta_{1,3} L^0$ peaks gives for p_M^x a value of $p_M^x = 0.18 \pm 0.03$ for Pd and $p_M^x = 0.18 \pm 0.04$ for La. This corresponds to an average number of M-shell holes of $m = 3.2 \pm 0.5$ for Pd and $m = 3.2 \pm 0.7$ for La, respectively.

The separate fit of the $K\alpha_{1,2} L^0$ peaks, on one hand, and of the $K\beta_{1,3} L^0$ peak, on the other, yields the values $p_M^x(K\alpha, \text{Pd}) = 0.12$, $p_M^x(K\beta, \text{Pd}) = 0.20$, $p_M^x(K\alpha, \text{La}) = 0.16$ and $p_M^x(K\beta, \text{La}) = 0.20$. The simultaneous fit gives certainly the most reliable value, since it takes into account different component shifts in the $K\alpha$ and $K\beta$ spectra. If the $K\alpha$ spectrum is fitted alone, the determination of p_M^x is difficult since the shift due to the removal of $3d$ electrons is very small (see Table II). Figures 2(a) and 2(b), and 3(a) and 3(b) show the detailed analysis of the $K\alpha L^0$ and $K\beta_{1,3} L^0$ lines of Pd and La with their M-satellite components. The measured L^0 lines are reproduced rather satisfactorily, but nevertheless the fitted curves seem to be slightly shifted ($K\alpha$ towards higher energies and $K\beta$ towards lower energies). These discrepancies can be attributed to unequal M-subshell ionization at the moment of the K x-ray transition (see Sec. IV C).

B. Average M-shell ionization at the moment of the ion-atom collision

The probability P_M^x reflects the number of holes in the M shell at the moment of the K x-ray transition. Although the decay of the K holes occurs very fast, several competitive processes may change the originally induced hole distribution. They can be accounted for by a statistical scaling procedure [36,37]. In our case, processes which produce one (LMX Auger and radiative L-M transitions) and two (LMM Auger) M-shell holes and processes which fill up M-shell vacancies (MXY Auger and radiative M transitions) are important. Note that the MMX Coster-Kronig transitions change the distribution between the subshells, but not the total number of M holes.

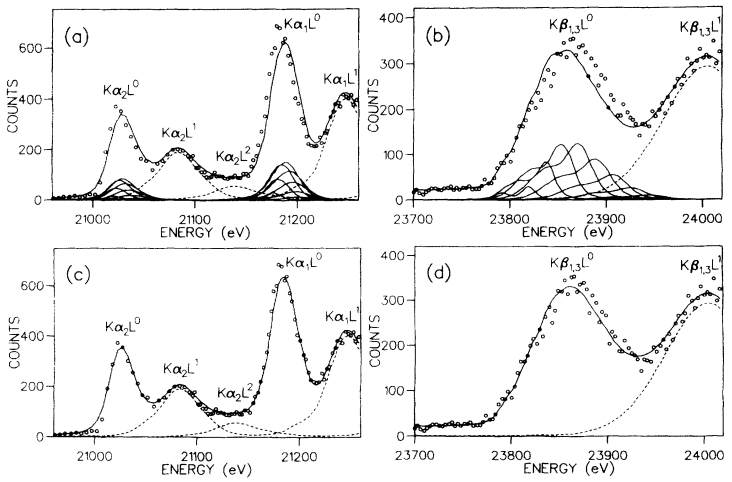

FIG. 2. Fitted L^0 lines of the Pd K x-ray spectra induced by 5.5-MeV/amu ^{16}O ions. (a) $K\alpha L^0$ lines fitted with one parameter p_M. The solid curves represent the $K\alpha L^0 M^m$ lines, the thick solid curve represents the sum of the $K\alpha L^0 M^m$ curves (all corresponding to the best fit value of p_M), and the dashed curve the simulated L^1 satellite line. (b) $K\beta_{1,3} L^0$ lines fitted with one parameter p_M. (c) $K\alpha L^0$ lines fitted with two parameters p_{3sp} and p_{3d}. (d) $K\beta_{1,3} L^0$ lines fitted with two parameters p_{3sp} and p_{3d}.

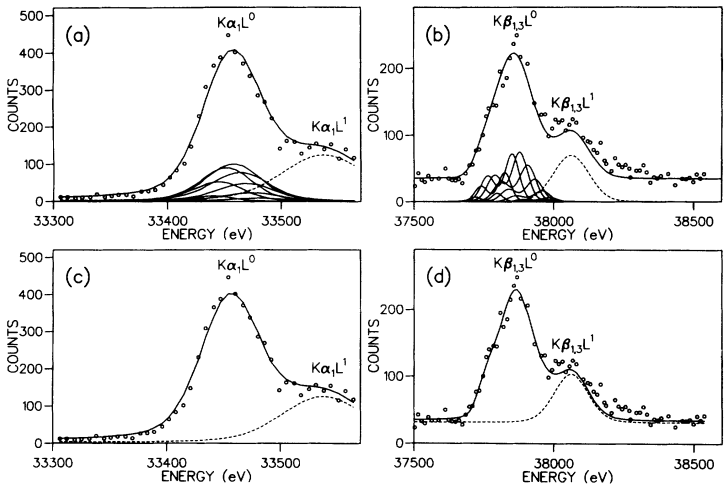

FIG. 3. Same as Fig. 2 but for La.

For La the *LLM* Coster-Kronig transition is energetically not possible. The rearrangement correction has been described in detail in Ref. [18]. The factor α [see Eq. (5) of Ref. [18]] is in our case $\alpha(\text{Pd})=0.51$ and $\alpha(\text{La})=0.32$.

Taking into account these corrections, the ionization probabilities per M-shell electron at the moment of the ion-atom collision are $p_M(\text{Pd})=0.17\pm0.03$ and $p_M(\text{La})=0.18\pm0.04$. The differences between the average M-shell ionization probabilities at the moment of the K x-ray transition and the ones at the moment of the ion-atom collision are thus rather small.

C. M-subshell ionization at the moment of the K x-ray emission

As mentioned above, the use of a single parameter for the M-shell ionization probability, equal for all subshells, gives a good but not a perfect fit. The same problem was encountered in a similar investigation of Mo [18]. Due to different subshell ionization probabilities and rearrangement processes the M subshells may be unequally ionized at the moment of the K x-ray transition. *MMX* Coster-Kronig transitions especially can transfer holes from the $3s$ or $3p$ subshells into $3d$ ones. The different binding energies of $3s$, $3p$, and $3d$ electrons and the different shape of their wave functions allow us to suppose that the subshells have different ionization probabilities.

For the ionization probability at the moment of the K x-ray transition two parameters, p^X_{3sp} and p^X_{3d}, were chosen. p^X_{3sp} represents the ionization probability for the $3s$ and $3p$ subshells and p^X_{3d} the one for the $3d$ subshells. For their determination a simultaneous fit of the $K\alpha L^0$ and $K\beta_{1,3}L^0$ lines is essential, since two parameters have to be determined. If the fits are carried out independently, unrealistic results are obtained, especially for the $K\alpha$ spectrum. By fitting $K\alpha$ and $K\beta_{1,3}$ simultaneously with two parameters it is possible to reproduce the experimental data in quite a satisfactory way [see Figs. 2(c), 2(d) and 3(c), 3(d)]. The probabilities obtained are $p^X_{3sp}(\text{Pd})=0.14\pm0.03$, $p^X_{3d}(\text{Pd})=0.25\pm0.03$ for palladium and $p^X_{3sp}(\text{La})=0.16\pm0.04$ and $p^X_{3d}(\text{La})=0.23\pm0.04$ for lanthanum.

D. M-subshell ionization at the moment of the ion-atom collision

In the case of distinguishable subshell ionization probabilities, the subshell dependence of the rearrangement corrections has to be taken into account. The $M_{sp}M_dX$ Coster-Kronig transitions especially change the occupation of the M subshells. These transitions transform $3s$ and $3p$ holes into $3d$ holes. Therefore, the ionization probability of the $3s$ and $3p$ subshells is higher at the moment of the ion-atom collision than at the moment of the K x-ray transition. For the $3d$ subshells it is the contrary. For $M_{sp}M_dX$ Coster-Kronig transitions the initial state must have necessarily a hole in the $3sp$ subshells. This condition is fulfilled in most of the Pd and La atoms since as mentioned above $p^X_{3sp}(\text{Pd})=0.14$ [i.e., the average number m_{3sp} of holes in the $3s$ and $3p$ subshells is about 1.1] and $p^X_{3sp}(\text{La})=0.16$ [i.e., $m_{3sp}(\text{La})=1.3$]. As the probability for an electron to be moved from the $3d$ subshells into the $3p$ or $3s$ subshells is proportional to the number of electrons and holes $(1-p_{3d})m_{3sp}$ present in the $3d$ and $3p$ or $3s$ subshells, respectively, the probability that such a $M_{sp}M_dX$ Coster-Kronig transition occurs before a K transition is given by

$$\frac{(1-p_{3d})m_{3sp}\Gamma_{M_{sp}M_dX}}{(1-p_{3d})m_{3sp}\Gamma_{M_{sp}M_dX}+\Gamma_K^m}, \tag{4}$$

where Γ_K^m is the K-shell width with m additional M-shell holes and $\Gamma_{M_{sp}M_dX}$ is the width of the $M_{sp}M_dX$ Coster-Kronig transition for singly ionized atoms. Calculated transition probabilities for singly ionized atoms are known [38–44].

In a similar way the other alternative transitions have to be taken into account. It should be reminded that L transitions can only occur if the initial state has an L-shell hole. Therefore, only atoms with one L-shell vacancy can change the M-shell hole distribution of the L^0 peak. The M-subshell ionization probabilities deduced from the measured values p^X_{3sp} and p^X_{3d} are for Pd: $p_{3sp}(\text{Pd})=0.17\pm0.3$, $p_{3d}(\text{Pd})=0.22\pm0.03$; for La:

p_{3sp}(La)=0.19±0.04, p_{3d}(La)=0.21±0.04. The change of the probabilities is again relatively small, so that the binomial distribution is only slightly influenced.

E. Error analysis

The specified error estimates are caused by the following:

(i) Calculated transition energies and measured x-ray energies are within 2 eV for Pd and 3 eV for La. Inaccuracies caused by errors in the relative yields of the calculated x-ray transition probabilities are assumed to be negligible. This assumption is based on the fact that for diagram lines the calculated yields correspond well with literature values. The absolute values of the transition probabilities have no influence, since we use the intensity scaling factor.

(ii) Errors resulting from the fitting procedure (including the statistics of the measured spectra).

(iii) Errors resulting from the rearrangement correction. We assumed a 10% error on the radiative and Auger widths.

An increase or decrease of the parameter p_M (or p_{3sp} and p_{3d}) produces a significant change of the theoretical line shape. Due to the simultaneous fit of the $K\alpha$ and $K\beta$ spectra, the determination of p_M is unique, resulting in an accurate value.

V. DISCUSSION

A. Other ionizing processes than direct Coulomb ionization

The capture of target electrons by the projectile may play an important role in the ionization process, depending on the electron binding energies and on the projectile energy. We have estimated the probability per M-shell electron of Pd and La to be captured by a bare oxygen projectile of 5.5 MeV/amu energy in a near-central collision, using an n-body classical trajectory Monte Carlo (nCTMC) program [45]. In the calculation we assumed the simplest version of the input, i.e., a three-body collision between the projectile and the target nucleus with charges Z_P and Z_T, respectively, and one electron, being initially in the M shell of the target atom. The experimental electron binding energy was used. The obtained values are $p_M^{\mathrm{EC}}(\mathrm{Pd})=(2.7\pm0.2)\times10^{-3}$ for Pd and $p_M^{\mathrm{EC}}(\mathrm{La})=(5.9\pm0.5)\times10^{-3}$ for La. The probabilities for electron capture are therefore much smaller than the measured ionization probabilities and the contribution of electron capture to the M-shell ionization can be neglected.

The removal of one or several inner-shell electrons causes a change of the central potential acting on the target electrons. Due to that change, electrons can be promoted to higher shells (shake up) or into the continuum (shake off). For the case of a K hole creation we have calculated the shake-off probability per M-shell electron probability per M-shell electron p_M^{shake} in the sudden approximation limit [46]. The calculated values are for Pd, $p_M^{\mathrm{shake}}(\mathrm{Pd})=1\times10^{-3}$ and for La, $p_M^{\mathrm{shake}}(\mathrm{La})=0.5\times10^{-3}$.

Target activation and Coulomb nuclear excitation can also contribute to additional K-shell ionization. These processes increase the intensity of the K diagram lines. The internal conversion of γ rays or the nuclear electron capture which follows the target activation, as well as the nuclear Coulomb excitation cause mainly a single primary inner-shell ionization. This is because the lifetimes of the nuclear states involved are much longer than those for the atomic transitions, so that an inner-shell vacancy is always filled prior to a subsequent nuclear transition [47]. In the measured spectra no significant increased intensity of the diagram transitions was observed. An estimation of the K-shell ionization cross section stemming from nuclear reaction processes has shown that these processes contribute less than 1% of the total K-shell ionization cross section.

The negligible influence on the inner-shell ionization of the above discussed ionizing processes and the relatively small change of the ionization probabilities by the rearrangement, show that the assumption of a binomial distribution of the M satellites at the moment of the K x-ray transition is a good approximation.

B. Calculation of the M-shell ionization probability

For a theoretical description of the ionization process caused by a charged projectile passing an atom, we may use the semiclassical approximation (SCA). The SCA model is a first-order perturbation theory, requiring that the collision is asymmetric, i.e, $Z_P<Z_T$. Z_P and Z_T are the atomic numbers of the projectile and the target, respectively. The reduced velocity η, i.e., the ratio of the projectile velocity to that of the target M-shell electron is given by

$$\eta=\frac{v_P}{v_M}=\left[\frac{E_P m_e}{U_M M_P}\right]^{1/2}, \tag{5}$$

where E_P is the beam energy, U_M is the average M-shell electron binding energy, and m_e and M_P are the electron and projectile masses, respectively. These ratios are $\eta(\mathrm{Pd})=2.6$ and $\eta(\mathrm{La})=1.7$, i.e., $\eta>1$, and therefore the SCA model is applicable.

The SCA theory is the only theory sufficiently developed to allow a detailed comparison with impact-parameter-dependent ionization probabilities. This theoretical model was originally introduced and developed by Bang and Hansteen [48] and co-workers. The SCA treatment has been shown to be very successful in the description of the K- and L-shell ionization by impact of light ions (e.g., [49–51] and references therein). The perturbed-stationary-state (ECPSSR) model of Brandt and Lapicki [52] incorporating energy-loss, Coulomb deflection, and relativistic corrections, is another successful theory for the description of the inner-shell ionization process. It gives, however, only total cross sections and no impact-parameter-dependent values. This theory is thus not suitable for a comparison with the measured ionization probabilities in near-central collisions.

The SCA version of Trautmann and Rösel [53] in a modified form [54] was used for the calculation of the

TABLE IV. Experimental and theoretical average M-shell ionization probabilities in near-central collisions of 5.5-MeV/amu ^{16}O ions with Pd and La atoms. p_M is the experimental average M-shell ionization probability per electron common for all M subshells and p_{3spd} the one obtained by taking the weighted average of p_{3sp} and p_{3d}. The theoretical values are calculated within the SCA model using relativistic hydrogenic (SCA-HYD) and Dirac-Hartree-Fock (SCA-DHF) wave functions.

Target	p_M	p_{3spd}	SCA-HYD	SCA-DHF
Pd	0.17±0.03	0.20±0.03	0.071	0.227
La	0.18±0.04	0.20±0.04	0.071	0.186

impact-parameter-dependent ionization probabilities. The main modification consists in the use of relativistic Hartree-Fock (DHF) wave functions instead of relativistic hydrogenic wave functions. This replacement seems to have a strong influence on the calculated values and brings the theoretical values in a much better agreement with the measured ones.

The calculations were performed using a classical hyperbolic trajectory including the recoil term. The latter may increase the M-shell ionization probability for zero impact parameter by a factor of 3 [12], however, for impact parameters $b \geq 50$ fm the recoil effect becomes negligible. The separated atom assumption was used and the multipole terms up to $L=5$ were included. The Dirac-Hartree-Fock (DHF) wave functions describing the bound atomic electrons and the continuum electrons were calculated with the use of the GRASP program [29] for bound electrons and the CONTWVG (continuum wave function solver for GRASP) program [55] for continuum electrons.

The experimental results are compared in Table IV with SCA calculations using relativistic hydrogenic (SCA-HYD) and Dirac-Hartree-Fock (SCA-DHF) wave functions. A weighted average of the calculated M-subshell ionization probabilities is used.

The M-subshell ionization probabilities are given in Table V. As one can see, the differences between the $3s$ subshell and the $3p$ subshells on one hand, and the $3d$ subshells on the other hand, are quite large. The weighted average for the $3s$, $3p$, subshells is for Pd, $p_{3sp}^{\text{SCA-DHF}}(\text{Pd})=0.16$ and for La, $p_{3sp}^{\text{SCA-DHF}}(\text{La})=0.12$. For the $3d$ subshells one has $p_{3d}^{\text{SCA-DHF}}(\text{Pd})=0.28$ and $p_{3sd}^{\text{SCA-DHF}}(\text{La})=0.24$. The corresponding experimental values are the following: $p_{3sp}(\text{Pd})=0.17\pm0.03$, $p_{3sp}(\text{La})=0.19\pm0.04$ $p_{3d}(\text{Pd})=0.22\pm0.03$, and $p_{3d}(\text{La})=0.21\pm0.04$.

The M-subshell ionization probabilities calculated with hydrogenic wave functions (see Table V) are almost identical. The effective charge of the target atom was calculated according to the Slater rule and the experimental binding energies were used. For the ones calculated with DHF wave functions differences of a factor of 2 exist between the $3s$ and $3d$ subshells. This shows the importance of using DHF wave functions in the calculation of the M-shell ionization.

The average experimental M-shell ionization probabilities calculated from the experimental subshell ionization probabilities are $p_{3spd}(\text{Pd})=0.20\pm0.03$ for Pd and $p_{3spd}(\text{La})=0.20\pm0.04$ for La, respectively. These values are slightly higher than the values obtained by fitting with only one parameter p_M. Since the two-parameter fit is better than the one-parameter fit, the p_{3spd} values are more realistic than the p_M ones and the calculated values should be compared with them. p_M seems to underestimate the ionization probability, which can be explained by the almost zero energy shift of the $K\alpha$ $3d$-satellite transitions. The ionization probability of the $3s$ and $3p$ subshells, which is smaller than the one of the $3d$ subshells, becomes in the fit important and has a considerable contribution to the determination of p_M.

It has to be mentioned that coupling effects [56,57] (for a review see [58]), which may change the subshell ionization probabilities noticeably [59,60] were not included in the calculation. It has been shown [56,61,62] that for not too symmetric collision systems the couplings in the con-

TABLE V. Experimental (Expt.) and calculated M-subshell ionization probabilities for collisions of 5.5 MeV/amu O projectiles on Pd and La targets and an impact parameter $b=500$ fm. For SCA-HYD hydrogenic wave functions were used and for SCA-DHF Dirac-Hartree-Fock wave functions were used.

Hole	Expt.	Calculated SCA-HYD	Calculated SCA-DHF
		Pd	
$3s_{1/2}$		0.065	0.137
$3p_{1/2}$	0.17±0.03	0.075	0.173
$3p_{3/2}$		0.071	0.175
$3d_{3/2}$	0.22±0.03	0.068	0.276
$3d_{5/2}$		0.068	0.276
		La	
$3s_{1/2}$		0.048	0.114
$3p_{1/2}$	0.19±0.04	0.081	0.119
$3p_{3/2}$		0.078	0.122
$3d_{3/2}$	0.21±0.04	0.071	0.241
$3d_{5/2}$		0.070	0.240

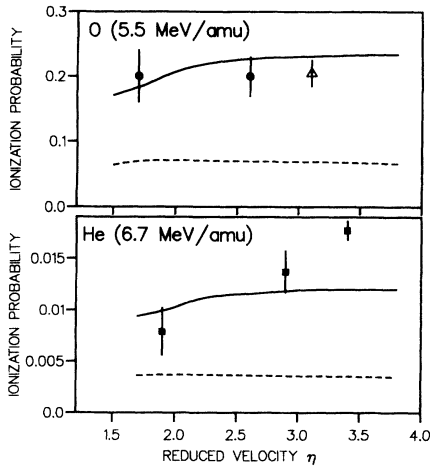

FIG. 4. Experimental and calculated ionization probabilities in near-central collisions of 5.5 MeV/amu O and 6.7-MeV/amu He ions with mid-Z target atoms. The dashed lines represent results of the SCA-HYD calculations. The solid lines those of the SCA-DHF calculations. Experimental values: ● this paper; △ from Ref. [18]; ■ from Ref. [17].

tinuum may be neglected. The M-shell ionization probability averaged over the M subshells should be therefore not substantially influenced by coupling effects. The calculated and measured M-subshell ionization probabilities should be compared only under the above-mentioned restriction.

C. Relevance of using DHF wave functions in the SCA calculation

The use of relativistic hydrogenic wave functions instead of relativistic Hartree-Fock wave functions seems to be the main reason for the discrepancies between the measured and the calculated average M-shell ionization probabilities in near-central collisions, observed in Refs. [17] and [18]. In the experiment described in Ref. [17], Mo, Pd, and La targets were bombarded by He^{2+} ions of 6.7-MeV/amu energy. From the x-ray satellite intensity yields the ionization probabilities for near-central collisions were deduced. A comparison with a SCA calculation using relativistic hydrogenic wave functions brought discrepancies up to a factor of 4 or more. Also in Ref. [18] (5.5-MeV/amu O ions on a Mo target) a discrepancy of a factor of 3 was observed. The measured M-shell ionization probabilities are plotted together with the results of this paper in Fig. 4. We have recalculated the M-shell ionization probabilities, using the SCA model with DHF wave functions. The differences in comparison with the ones calculated with relativistic hydrogenic wave functions are substantial. They are also shown in Fig. 4.

Recently, Rymuza *et al.* [63] and Anagnostopoulos *et al.* [64] have pointed out the importance of using Hartree-Fock–type wave functions also for describing the L-shell ionization probabilities in near-central collisions. The latter have shown that the measured lanthanum K x-ray spectra induced by the bombardment with 403-MeV nitrogen could be much better reproduced theoretically by using wave functions from a variationally determined optimized potential than screened relativistic hydrogenic ones. This potential gives wave functions which are similar to Hartree-Fock wave functions [65]. For the L-subshell ionization differences up to a factor of 2 were found.

VI. SUMMARY

The essential goal of this paper is the verification of our recently presented (Ref. [18]) method of analysis of complex spectra by using two targets differing by their Z value. Although in the measured K x-ray spectra the M satellite transitions are not resolved, it is nevertheless possible to determine the M-shell ionization probability. In collisions of 5.5-MeV/amu oxygen ions with Pd and La, electron capture from the M-shell, M-shell electron shake-off, and K-shell ionization by target activation play a minor role compared with the direct Coulomb ionization. Thus, the M-shell hole distribution can be approximated by a binomial one. In the case of not too different M-subshell ionization probabilities, the binomial distribution is governed by a single-parameter p_M^x, the average ionization probability per M-shell electron at the moment of the K x-ray transition. However, the M-subshell ionization probabilities are different. Therefore in the analysis of the K x-ray spectra we introduced two different ionization probabilities, p_{3sp}^X for the $3s$ and $3p$ subshells and p_{3d}^X for the $3d$ subshells, respectively. In consequence a considerable improvement of the fit was achieved. Taking into account the rearrangement processes, the ionization probabilities at the moment of the K x-ray transition were converted to ionization probabilities at the moment of the ion-atom collision.

SCA calculations have shown that if Dirac-Hartree-Fock instead of screened hydrogenic wave functions are used, a much better agreement with the experiment is obtained. This demonstrates that for the M-shell ionization the use of wave functions from self-consistent calculations with respect to the inner screening is relevant. It should be mentioned that the coupling effect has not been included in our calculations, but the possible error due to this omission has been estimated to be small.

ACKNOWLEDGMENTS

This work was supported in part by the Swiss National Science Foundation, the Paul Scherrer Institute PSI (formerly SIN), as well as the Polish Committee for Scientific Research (KBN). The authors are grateful to Dr. Stammbach and Dr. Schmelzbach and the cyclotron crew for good beam conditions. They would like to thank Professor D. Trautmann for making his program available for performing ionization-probability calculations.

[1] J. Reinhard, W. Greiner, J. Greenberg, and P. Vincent, in *Treatise of Heavy Ion Science,* edited by A. Bromley (Plenum, New York, 1985), Vol. 5.
[2] T. J. Gray, in *Methods of Experimental Physics,* edited by P. Richard (Academic, New York, 1980), Vol 17, p. 193.
[3] H. Paul and J. Muhr, Phys. Rep. **135**, 47 (1986).
[4] D. Trautmann and Th. Kauer, Nucl. Instrum. Methods B **42**, 449 (1989).
[5] R. S. Sokhi and D. Crumpton, At. Data Nucl. Data Tables **30**, 49 (1984); J. Phys. B **18**, 2871 (1985).
[6] E. Braziewicz and J. Braziewicz, J. Phys. B **21**, 1537 (1988).
[7] M. Pajek, A. P. Kobzev, and G. Lapicki, Nucl. Instrum. Methods B **48**, 87 (1990).
[8] A. Bienkowski, J. Braziewicz, T. Czyzewski, L. Glowacka, M. Jaskola, G. Lapicki, and M. Pajek, Nucl. Instrum. Methods B **49**, 19 (1990).
[9] M. Pajek, A. P. Kobzev, R. Sandrik, A. V. Skrypnik, R. A. Ilkhamov, S. H. Khusmurodov, and G. Lapicki, Phys. Rev. A **42**, 261 (1990).
[10] A. P. Jesus and J. P. Ribeiro, Nucl. Instrum. Methods A **280**, 370 (1989).
[11] G. Lapicki, J. Phys. B **23**, 3123 (1990).
[12] M. Carlen, J.-Cl. Dousse, M. Gasser, J. Kern, Ch. Rhême, P. Rymuza, Z. Sujkowski, and D. Trautmann, Europhys. Lett. **13**, 231 (1990).
[13] B. Perny, J.-Cl. Dousse, M. Gasser, J. Kern, R. Lanners, Ch. Rhême, and W. Schwitz, Nucl. Instrum. Methods A **267**, 120 (1988).
[14] N. Stolterfoht, Phys. Scr. **42**, 192 (1990).
[15] J. O. P. Pedersen, Phys. Scr. **42**, 180 (1990).
[16] J. F. Reading and A. L. Ford, Comm. At. Mol. Phys. **23**, 301 (1990).
[17] M. Carlen, J.-Cl. Dousse, M. Gasser, J. Hoszowska, J. Kern, Ch. Rhême, P. Rymuza, Z. Sujkowski, and D. Trautmann, Z. Phys. D **23**, 71 (1992).
[18] M. W. Carlen, M. Polasik, B. Boschung, J.-Cl. Dousse, M. Gasser, Z. Halabuka, J. Hoszowska, J. Kern, B. Perny, Ch. Rhême, P. Rymuza, and Z. Sujkowski, Phys. Rev. A **46**, 3893 (1992).
[19] J.-Cl. Dousse and J. Kern, Acta Crystallogr. A **36**, 966 (1980).
[20] S. I. Salem and P. L. Lee, At. Data Nucl. Tables **18**, 233 (1976).
[21] B. Jeckelmann *et al.*, Nucl. Instrum. Methods A **241**, 191 (1985).
[22] J. D. Sevier, At. Data Nucl. Data Tables **24**, 323 (1979).
[23] I. P. Grant, B. J. McKenzie, P. H. Norrington, D. F. Mayers, and N. C. Pyper, Comput. Phys. Commun. **21**, 207 (1980).
[24] B. J. McKenzie, I. P. Grant, and P. H. Norrington, Comput. Phys. Commun. **21**, 233 (1980).
[25] I. P. Grant and B. J. McKenzie, J. Phys. B **13**, 2671 (1980).
[26] J. Hata and I. P. Grant, J. Phys. B **16**, 3713 (1983).
[27] I. P. Grant, Int. J. Quantum Chem. **25**, 23 (1984).
[28] I. P. Grant, J. Phys. B **7**, 1458 (1974).
[29] K. G. Dyall, I. P. Grant, C. T. Johnson, F. A. Parpia, and E. P. Plummer, Comput. Phys. Commun. **55**, 425 (1989).
[30] M. Polasik *et al.* (unpublished).
[31] B. Perny, J.-Cl. Dousse, M. Gasser, J. Kern, Ch. Rhême, P. Rymuza, and Z. Sujkowski, Phys. Rev. A **36**, 2120 (1987).
[32] O. Benka, R. L. Watson, K. Parthasaradhi, J. M. Sanders, and R. J. Maurer, Phys. Rev. A **27**, 149 (1983).
[33] R. L. Watson, A. K. Leeper, B. I. Sonobe, T. Chiao, and F. E. Jenson, Phys. Rev. A **15**, 914 (1977).
[34] J. A. Demarest and R. L. Watson, Phys. Rev. A **17**, 1302 (1978).
[35] T. M. Rosseel, J. M. Dale, H. W. Dunn, L. D. Hulett, Jr., S. Kahane, H. F. Krause, S. Raman, G. G. Slaughter, C. R. Vane, and J. P. Young, Nucl. Instrum. Methods B **3**, 94 (1984).
[36] F. P. Larkins, J. Phys. B **4**, L29 (1971).
[37] P. Rymuza, Z. Sujkowski, M. Carlen, J.-Cl. Dousse, M. Gasser, J. Kern, B. Perny, and Ch. Rhême, Z. Phys. D **14**, 37 (1989).
[38] E. J. McGuire, Phys. Rev. A **3**, 587 (1971).
[39] E. J. McGuire, Phys. Rev. A **5**, 1043 (1972); **5**, 1052 (1972).
[40] J. H. Scofield, At. Data Nucl. Data Tables **14**, 121 (1974).
[41] O. Keski-Rahkonin and M. O. Krause, At. Data Nucl. Data Tables **14**, 139 (1974).
[42] M. H. Chen, B. Crasemann, and H. Mark, At. Data Nucl. Data Tables **24**, 13 (1979).
[43] M. H Chen, B. Crasemann, and H. Mark, Phys. Rev. A **21**, 436 (1980).
[44] M. H. Chen, B. Crasemann, and H. Mark, Phys. Rev. A **24**, 177 (1981).
[45] R. E. Olson, in *Electronic and Atomic Collisions,* edited by H. B. Gilbody, W. R. Newell, F. H. Read, and A. C. H. Smith (Elsevier, New York, 1988), p. 271.
[46] T. A. Carlson and C. W. Nestor, Phys. Rev. A **8**, 2887 (1973).
[47] Z. Sujkowski, in *Coherent Effects in Highly Excited Nuclei,* edited by Z. Wilhelmi and G. Szeflinska (Harwood, New York, 1987).
[48] J. Bang, J. M. Hansteen, K. Dan. Vidensk. Selsk. Mat. Fys. Medd. **31**, No. 13 (1959).
[49] M. Pajek, A. P. Kobzev, D. Trautmann, and Th. Kauer, Nucl. Instrum. Methods B **52**, 109 (1990).
[50] J. M. Hansteen, L. Kocbach, and A. Graue, Phys. Scr. **31**, 63 (1985).
[51] E. Braziewicz, J. Braziewicz, T. Czyzewski, L. Glowacka, M. Jaskola, T. Kauer, A. P. Kobzev, M. Pajek, and D. Trautmann, J. Phys. B **24**, 1669 (1991).
[52] W. Brandt and G. Lapicki, Phys. Rev. A **20**, 465 (1979); **23**, 1717 (1981).
[53] D. Trautmann and F. Rösel, Nucl. Instrum. Methods **169**, 259 (1980).
[54] Z. Halabuka, W. F. Perger, and D. Trautmann, Z. Phys. D (to be published).
[55] W. F. Perger, Z. Halabuka, and D. Trautmann, Comput. Phys. Commun. **76**, 250 (1993).
[56] G. Mehler, J. Reinhardt, B. Müller, W. Greiner, and G. Soff, Z. Phys. D **5**, 143 (1987).
[57] P. A. Amundsen and D. H. Jakubassa-Amundsen, J. Phys. B **21**, L99 (1988).
[58] D. Trautmann and G. Baur, Nucl. Instrum. Methods B **40/41**, 345 (1989).
[59] L. Sarkadi and T. Mukoyama, J. Phys. B **14**, L255 (1981); Nucl. Instrum. Methods **232**, 296 (1984); J. Phys. B **20**, L559 (1987).
[60] L. Sarkadi, J. Phys. B **19**, 2519 (1986).
[61] M. H. Martir, A. L. Ford, J. F. Reading, and R. L. Becker, J. Phys. B **15**, 2405 (1982).
[62] G. Mehler, T. de Reus, U. Müller, J. Reinhardt, B. Müller, W. Greiner, and G. Soff, Nucl. Instrum. Methods A **240**, 559 (1985).
[63] P. Rymuza, T. Ludziejewski, Z. Sujkowski, M. Carlen, J.-

Cl. Dousse, M. Gasser, J. Kern, and Ch. Rhême, Z. Phys. D **23**, 81 (1992).
[64] D. F. Anagnostopoulos, G. L. Borchert, and D. Gotta, J. Phys. B **25**, 2771 (1992).
[65] K. Aashamar, T. M. Luke, and J. D. Talman, At. Data Nucl. Data Tables **15**, 305 (1978).
[66] J. A. Bearden, Rev. Mod. Phys. **39**, 78 (1967).